



# Definition of a temporal distribution index for high temporal resolution precipitation data over Peninsular Spain and the Balearic Islands: the fractal dimension; and its synoptic implications

Oliver Meseguer-Ruiz<sup>1,7</sup> · Timothy J. Osborn<sup>2</sup> · Pablo Sarricolea<sup>3</sup> · Philip D. Jones<sup>2,4</sup> · Jorge Olcina Cantos<sup>5</sup> · Roberto Serrano-Notivoli<sup>6</sup> · Javier Martin-Vide<sup>7</sup>

Received: 3 June 2017 / Accepted: 15 February 2018 / Published online: 8 March 2018  
© Springer-Verlag GmbH Germany, part of Springer Nature 2018

## Abstract

Precipitation on the Spanish mainland and in the Balearic archipelago exhibits a high degree of spatial and temporal variability, regardless of the temporal resolution of the data considered. The fractal dimension indicates the property of self-similarity, and in the case of this study, wherein it is applied to the temporal behaviour of rainfall at a fine (10-min) resolution from a total of 48 observatories, it provides insights into its more or less convective nature. The methodology of Jenkinson & Collinson which automatically classifies synoptic situations at the surface, as well as an adaptation of this methodology at 500 hPa, was applied in order to gain insights into the synoptic implications of extreme values of the fractal dimension. The highest fractal dimension values in the study area were observed in places with precipitation that has a more random behaviour over time with generally high totals. Four different regions in which the atmospheric mechanisms giving rise to precipitation at the surface differ from the corresponding above-ground mechanisms have been identified in the study area based on the fractal dimension. In the north of the Iberian Peninsula, high fractal dimension values are linked to a lower frequency of anticyclonic situations, whereas the opposite occurs in the central region. In the Mediterranean, higher fractal dimension values are associated with a higher frequency of the anticyclonic type and a lower frequency of the advective type from the east. In the south, lower fractal dimension values indicate higher frequency with respect to the anticyclonic type from the east and lower frequency with respect to the cyclonic type.

**Keywords** Precipitation · Fractal dimension · Jenkinson & Collinson · Weather types · Iberian Peninsula · Western Mediterranean

✉ Oliver Meseguer-Ruiz  
omeseguer@academicos.uta.cl

- <sup>1</sup> Departamento de Ciencias Históricas y Geográficas, Universidad de Tarapacá, 2222, 18 de septiembre, Arica, Chile
- <sup>2</sup> Climatic Research Unit, School of Environmental Sciences, University of East Anglia, Norwich, UK
- <sup>3</sup> Department of Geography, University of Chile, Santiago, Chile
- <sup>4</sup> Center of Excellence for Climate Change Research, Department of Meteorology, King Abdulaziz University, Jeddah 21589, Saudi Arabia
- <sup>5</sup> Interuniversity Institute of Geography, University of Alicante, Alicante, Spain
- <sup>6</sup> Barcelona Supercomputing Center, Barcelona, Spain
- <sup>7</sup> Climatology Group, University of Barcelona, Barcelona, Spain

## 1 The temporal fractality of precipitation

The analysis of temporal variability with respect to climatic components in general is one of the issues which receives much attention in contemporary climatic studies; specifically, precipitation appears as a principal focus of studies in the Iberian Peninsula (Casanueva et al. 2014; De Luis et al. 2010; Gonzalez-Hidalgo et al. 2009; Goodess and Jones 2002; Martin-Vide and Lopez-Bustins 2006; Ramos et al. 2016; Rodríguez-Puebla and Nieto 2010; Rodríguez-Solà et al. 2016; Sáenz et al. 2001, among others). This interest originates from the exigent need to distinguish between natural climatic variability and anthropogenically-induced phenomena. We can speak of climate change not only in terms of a statistically significant increase or decrease in the average of a climate-related parameter, but also whether there is a significant change in variability.

The influence of the Mediterranean Sea is a vital factor in atmospheric processes affecting the Iberian Peninsula, as it plays a major role by introducing peculiarities to the study area. Due to its location and size, the Mediterranean is very sensitive and responds quickly to atmospheric forcing (Lionello 2012). In addition, its western region, which includes the Iberian Peninsula, is affected by a marked inter-annual variability in precipitation, wherein wet years alternate with very dry years (Vicente-Serrano et al. 2011; Trigo et al. 2013), which gives the study area a strong climatic personality. Despite the trends in recent decades, which indicate that the southeaster area of this region is heading toward a more arid climate (Del Río et al. 2011; González-Hidalgo et al. 2003), it is not free from extreme events with precipitation of a high hourly intensity which has serious consequences at the socio-economic level (Liberato 2014; Trigo et al. 2015). Moreover, Iberia's geography with the Mediterranean to the east means that Southeast Spain gets more rain with easterly winds (Martín-Vide 2004).

As in the case of fractal objects, processes and systems that remain invariant with a change of scale are not defined by any particular scale. A fractal process is one in which the same basic process takes place at different levels; these levels, in turn, reproduce the entire process (Mandelbrot 1977). The application of these principles has facilitated the description of complex objects and processes which are already widely used and accepted in many fields of the natural sciences including geography, ecology, and new technologies applied to regional information (Goodchild 1980; Goodchild and Mark 1987; Hastings and Sugihara 1994; Peitgen et al. 1992; Tuček et al. 2011). Due to the fractal behaviour of some atmospheric variables (temperature, precipitation, and atmospheric pressure), fractal analysis has been used in climatic studies to determine the persistence of these variables and their interdependencies (Nunes et al. 2013; Rehman 2009).

Other indicators can be used to define dynamical systems. The Lyapunov exponent (Wolf et al. 1985; Wolf 2014) indicates chaos when large and positive, but this application is difficult, even impossible for experimental data records. (Sprott 2003). The fractal dimension can also directly be determined considering the Hurst exponent applied to self-affine series, and is a measure of a data series randomness (Amaro et al. 2004; Malinverno 1990). More recently, other studies have been developed around atmospheric flows that consider the well-known large-scale patterns (ENSO, PDO, NAO...) combined with the chaotic dynamics: the local dimension (Faranda et al. 2017). According to these papers, it seems that these local dimensions are able to represent specific circulation patterns related to time series extreme events.

For some years, these principles have been applied to the spatial distribution of precipitation, rather than its temporal

distribution based on an intuitive assumption that a precipitation field may take the form of a fractal object, as it complies with the criterion of self-similarity (Lovejoy and Mandelbrot 1985). When referring to the temporal fractality of precipitation, the concept becomes more abstract; scaling is applied to the duration of the interval for which the occurrence or absence of recorded precipitation is verified, and the same process is repeated at intervals of shorter and longer duration. The purpose of this is to ascertain whether the property of self-similarity is maintained when considering different temporal resolutions.

Several applications have been developed in various disciplines, such as hydrology, from the fractal properties of the spatial and temporal distribution of precipitation (Zhou 2004; Khan and Siddiqui 2012). These fractal processes have been identified in a study on the Spanish mainland from series of accumulated precipitation spanning 90 years, and its analysis demonstrates that its distribution is consistent with fractal distribution as explained in other study (Oñate Rubalcaba 1997). The values obtained, with an average fractal dimension of 1.32 for the whole territory, are in the same order of magnitude as the fractal dimensions obtained from other macrometeorological and palaeoclimatic records. Fractal analysis also facilitates the identification of trends based on the Mann–Kendall test. One example is the study conducted in the province of La Pampa (Argentina), where this analysis defines trends in more detail than the projections carried out by the IPCC-AR4 (Pérez et al. 2009). In Venezuela, it has been possible to predict climate changes at different temporal scales based on the same fractal methodology (Amaro et al. 2004). Fractal analysis was also used in studies that have evaluated precipitation trends in regions of the world where access to water is becoming increasingly scarce in parallel with exponential economic growth in recent years (Rehman and Siddiqi 2009; Gao and Hou 2012). However, the application of this analytical method to regions with precipitation of very high hourly intensity has exhibited deficiencies. In these cases, extreme precipitation events conform to models which are even more complex than multifractal models, and which consider not only the occurrence of the phenomenon, but also the recorded quantities, which are affected by very short durations and very high return periods (Dunkerley 2008; García-Marín et al. 2008; Langousis et al. 2009; Veneziano et al. 2006). The importance of the temporal resolution of existing data is particularly apparent in the fractal analysis, as the availability of both hourly and daily data results in significant changes in the values of both the increasing and decreasing fractal dimensions (García-Marín 2007; López Lambrano 2014). Another application is the regionalisation of a territory based on a fractal analysis of the temporal distribution of precipitation (Dunkerley 2010; Reiser and Kutiel 2010; Kutiel and Trigo 2014). These studies usually lack references to the

mechanisms generating the rainfall under consideration, but it has been found that their results are directly linked to local and regional characteristics, particularly the synoptic origins of precipitation, with an influence on the fractal dimension (Rodríguez et al. 2013; Meseguer-Ruiz and Martín-Vide 2014). It has also been possible to determine, with satisfactory results, the relationship of the fractal dimension with other indices of temporal variability in precipitation, whose significance is well known (coefficient of variation, concentration index, etc.), again as a function of the temporal resolution of the baseline data (Meseguer-Ruiz et al. 2017b).

Ghanmi et al. (2013) performed a study in the eastern Mediterranean based on precipitation series with high temporal resolution and have identified three types of temporal structures from Hurst's analysis. The temporal fractality of precipitation in another nearby area, Veneto (Italy), was compared with that of precipitation in the Ecuadorian Amazon province of Pastaza (Kalauzi et al. 2009), and it was concluded that the temporal behaviour of the precipitation events of the two regions are opposite, with decreasing trends in the former case, and increasing trends in the latter. In the western Mediterranean, on the Iberian Peninsula,

the highest fractal dimension values have been obtained in areas with greater quantities of precipitation (Meseguer-Ruiz et al. 2017a). Fractal analysis has also been applied in a very different climatic environment, in India, demonstrating the effect of the monsoon on fractal dimension values (Selvi and Selvaraj 2011). In Queensland, Australia, Breslin and Belward (1999) calculated the fractal dimension of monthly series of precipitation from a methodology based on models for the prediction of cumulative quantities.

The aim of this study is to give a synoptic significance to this new indicator of temporal variability in precipitation, which is the fractal dimension, by determining what types of situations at the surface and above ground (500 hPa) are associated with certain values of FD.

## 2 Data and methodology

The study was carried out using precipitation data at a resolution of 10 min from the databases of 48 observatories in the Spanish Meteorological Agency's (AEMET) network of automatic stations (Fig. 1). There were initially a total of 75

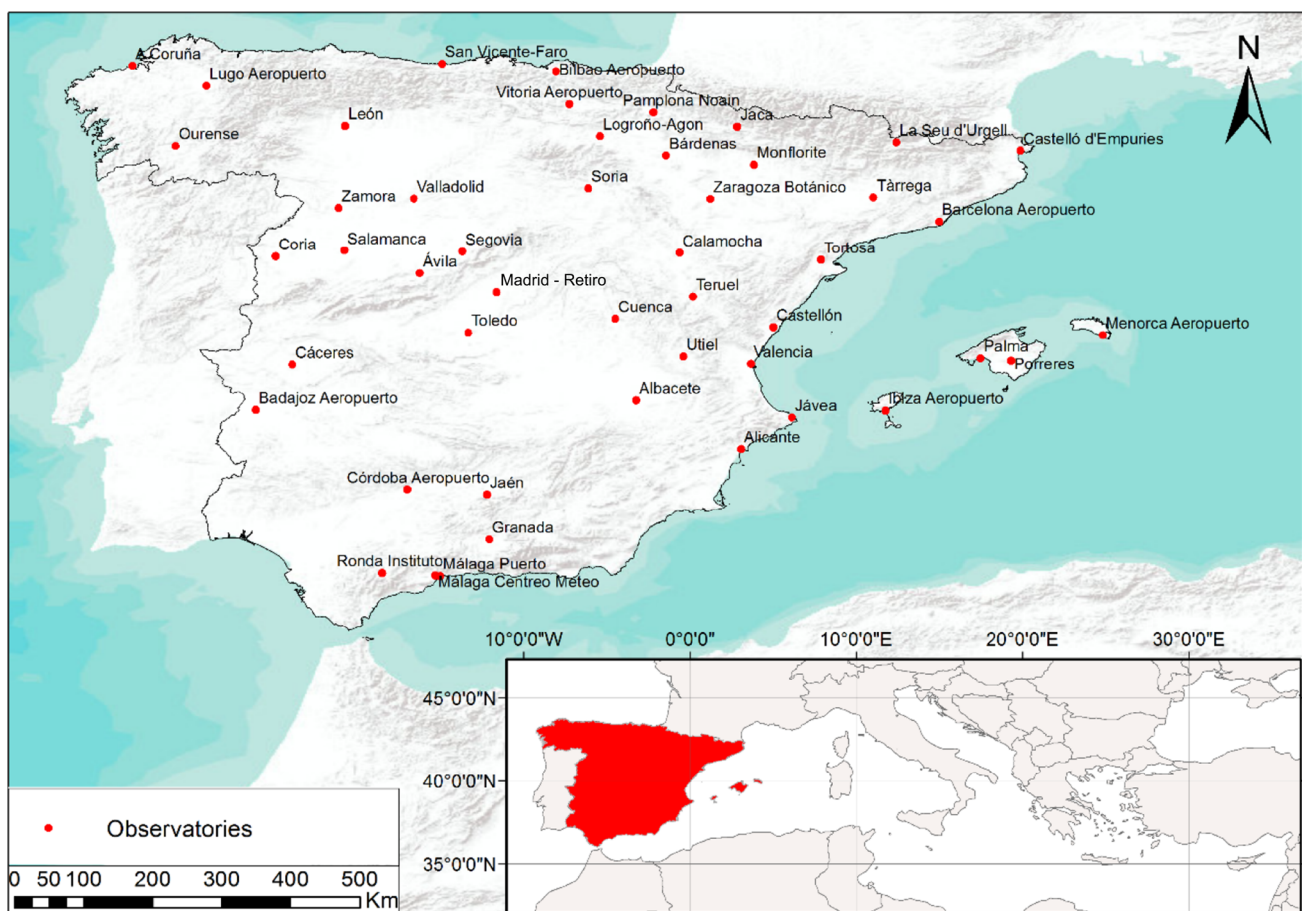


Fig. 1 Location of the observatories used in the study

observatories, but series with missing values of more than 15% were discarded. Values appearing as outliers, i.e. those which were too high to record in 10 min, those higher than 1.5 times the third quartile, were also eliminated in order to maintain the homogeneity of the series to the greatest extent possible. The total number of values eliminated this way has no significant effects on the results (less than 0.5% of the whole data). Due to the high temporal resolution of the series, no filling method has been applied.

Moreover, a common period was selected for observatories whose series offer guaranteed quality and homogeneity, based on the manual elimination of those records that are out of range, this being the period between 1995 and 2010.

The calculation of the fractal dimension (FD) was performed according to the box-counting method in the following manner: rainfall records with a 10-min resolution were used, as the 10-min period is the unit interval which served as the basis for performing the analysis. Then, periods containing 1, 2, 3, 6, 12, 18, 24, 36, 48, 72, 144 and 288 unit intervals, i.e. periods of 10, 20 and 30 min, 1, 2, 3, 4, 6, 8, 12, 24 and 48 h, respectively, were established and the number of those which had some amount of precipitation was tallied and recorded. The utilisation of 10-min intervals for 2 days reflects the intention of studying the occurrence or absence of precipitation on small time scales. The fractal dimension value of the temporal distribution of precipitation is defined on the basis of the slope of the regression line resulting from representing pairs of values obtained from the natural logarithms of  $l$ , length of the interval in hours, and  $N$ , number of intervals with precipitation. In fact, the natural logarithms of these pairs of values for each observatory are aligned with remarkable proximity. The fractal dimension FD is given by  $1 + \alpha$ , where  $\alpha$  is the absolute value of the slope of the regression line (Fig. 2). The regression lines for obtaining the FD values at the Ibiza and Lugo observatories are presented by way of illustration.

To ensure that the FD results were correct and within proper confidence intervals, a goodness-of-fit analysis was

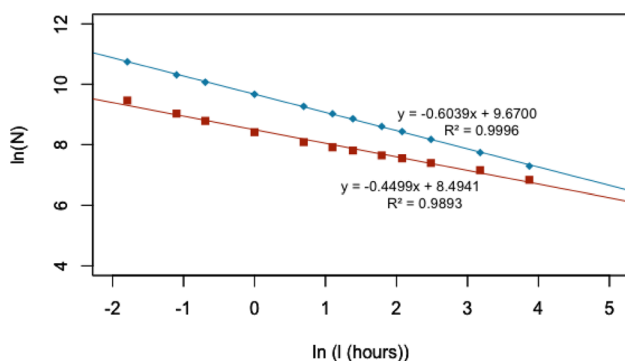


**Fig. 2** Regression lines for obtaining FD values in Ibiza (red) and Lugo (blue) during the period from 1997 to 2010

applied by generating several realizations of surrogate data of the same length as the original series. For each station, we simulated  $100 \times n_{\text{years}}$  series of  $N$  with mean and standard deviation the mean and deviation of each  $l$ -interval. For instance, for a station with 17 years of original data we generated  $100 \times 17$  values of  $N$  in each  $l$ -interval, producing 1700 simulated annual series with the same structure as the original ones. These series were used to compute their corresponding FD values and then compared with the original through the calculation of mean error (ME), mean absolute error (MAE) and the root mean squared error (RMSE).

Next, a cluster analysis of the 48 observatories, which enabled the differentiation of observatories into four groups as a function of latitude, longitude and FD value, was carried out, and a representative observatory having the best temporal series (with fewest missing values) was selected from each of these groups. The decision on choosing four groups is based on the conclusions obtained in a previous study, where four regions were identified according to a subjective criteria (Meseguer-Ruiz et al. 2017a).

As this grouping could mainly depend on the geographical location of the stations and less on the FD values, the cluster analysis was reanalysed 1000 times by randomly rearranging the FD corresponding to each location and keeping the latitude and longitude. These resulting clusters assignments were compared with the original by summarizing the coincidences of the groups by station and by clusters.

Moreover, the synoptic classification of Jenkinson & Collison (J&C) (1977) is an automated method which facilitates the determination of the type of atmospheric circulation from atmospheric pressure reduced to sea level at 16 points (Fig. 3). It is based on the classification of Lamb (1972) and his LWT (Lamb Weather Types) and also proposes J&C weather types (J&CWT) which were developed by Jones et al. (1993).

In recent years, there have been several studies which have applied the methodology of Jenkinson & Collison (J&C) to various study areas, including the Iberian Peninsula (Grimalt et al. 2013; Martín-Vide 2002; Spellman 2000; Trigo and DaCamara 2000); however, it is not the only synoptic classification that has been applied in this region, as demonstrated by the completion of the COST 733 action for the European continent (Philipp et al. 2014) and various regions of the world outside of the inter-tropical and polar areas, as is the case for Scandinavia, Central Europe, Russia, the United States and Chile (Esteban et al. 2006; Linderson 2001; Pepin et al. 2011; Post et al. 2002; Sarricolea et al. 2014, 2017; Soriano et al. 2006; Spellman 2016; Tang et al. 2009).

The J&C classification has frequently been used to synoptically characterise variations in different climatic variables with temperature, precipitation and wind being the most studied (Goodess and Jones 2002; Osborn et al. 1999), but



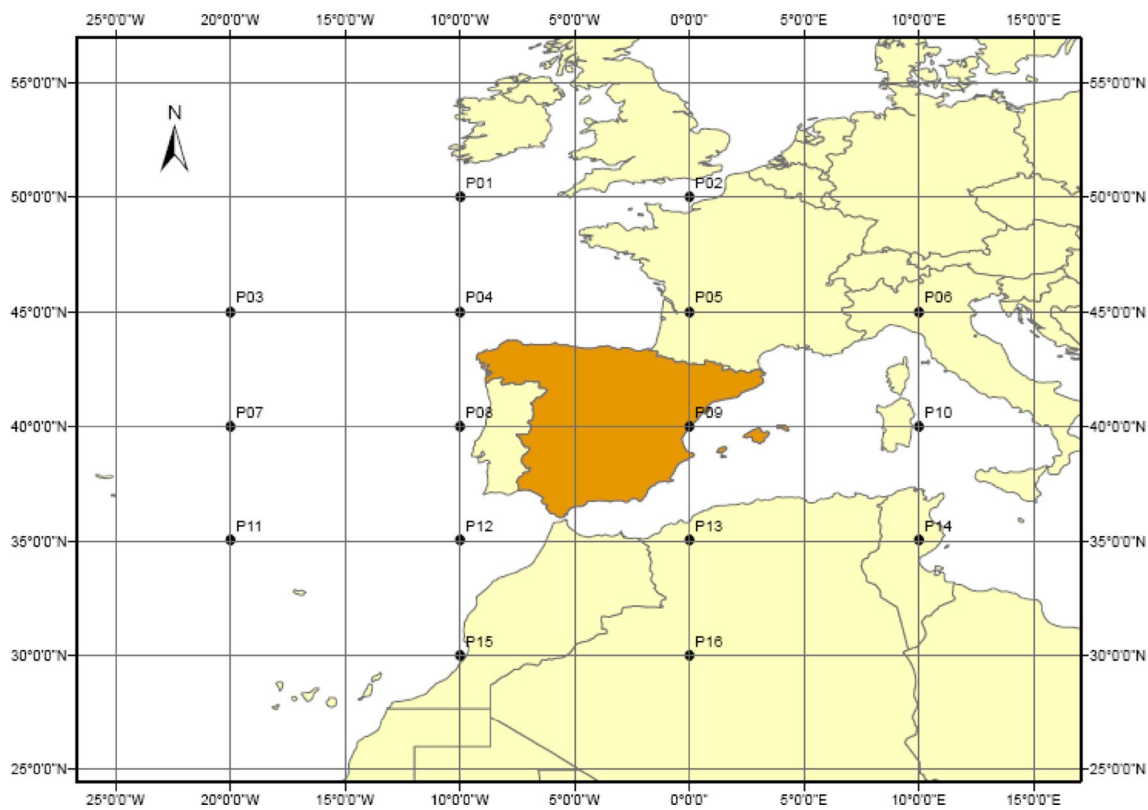


**Fig. 3** 16-point grid for obtaining the J&C weather types

it is also used in climatic modelling for analysing the pressure fields and the simulated deposition of mineral powder (Demuzere and Werner 2006).

However, whenever an attempt has been made to relate the precipitation variable with specific synoptic situations, what has been successfully demonstrated is, for example, the conditions under which a greater amount of precipitation accumulates, or the situations in which more persistent rainfall conditions appear (Martín-Vide et al. 2008). Nevertheless, synoptic climatology at a high temporal resolution (4 times per day, every 6 h) has yet to be correlated with any indicators of the temporal regularity or irregularity of precipitation in the Iberian Peninsula in order to provide climatic and geographical coherence to these results which indicate the temporal behaviour of precipitation, as has been done in the United Kingdom (Osborn and Jones 2000).

A 16-point grid (Fig. 3) was chosen in order to enable a better assessment of the Mediterranean and Atlantic influences on the synoptic types which affect the study area. The atmospheric pressure data for this study were obtained for the 1995–2010 ERA Interim (Dee et al. 2011) project, at a resolution of 6 h at 00:00, 06:00, 12:00 and 18:00 UTC. This reanalysis database was selected, because it offers a better correlation with the classification of weather types than other products (Jones et al. 2013).

The J&C classification consists of 27 weather types: 8 purely advective (N, NE, E, SE, S, SW, W and NW), 1 cyclonic (C), 1 anticyclonic (A), 8 advective-cyclonic hybrids (CN, CNE, CE, CSE, CS, CSW, CW and CNW), 8 advective-anticyclonic hybrids (AN, ANE, AE, ASE, AS, ASW, AW and ANW) and 1 indeterminate (U).

The variables which need to be calculated for the application of the J&C method are the zonal component of the geostrophic wind ( $W$ ) (in our case between  $35^\circ$  and  $45^\circ\text{N}$ ), the meridional component of the geostrophic wind ( $S$ ) (in our case between  $20^\circ\text{W}$  and  $10^\circ\text{E}$ ), the wind direction ( $D$ ) in azimuthal degrees, the wind speed in m/s ( $F$ ), the zonal component of vorticity ( $Z_w$ ), the meridional component of vorticity ( $Z_s$ ) and total vorticity ( $Z$ ).

The analytical expressions adjusted for the Iberian Peninsula are as follows:

$$W = 0.5(P_{12} + P_{13}) - 0.5(P_4 + P_5)$$

$$S = 1.3052[0.25(P_5 + 2P_9 + P_{13}) - 0.25(P_4 + 2P_8 + P_{12})]$$

$$F = \sqrt{W^2 + S^2}$$

$$D = \tan^{-1}\left(\frac{W}{S}\right)$$

$$Z_w = 1.1207 \left[ \frac{1}{2}(P_{15} + P_{16}) - \frac{1}{2}(P_8 + P_9) \right] - 0.909 \left[ \frac{1}{2}(P_8 + P_9) - \frac{1}{2}(P_1 + P_2) \right]$$

$$Z_s = 0.852 \left[ \frac{1}{4}(P_6 + 2P_{10} + P_{14}) - \frac{1}{4}(P_5 + 2P_9 + P_{13}) - \frac{1}{4}(P_4 + 2P_8 + P_{12}) + \frac{1}{4}(P_3 + 2P_7 + P_{11}) \right]$$

$$Z = Z_w + Z_s$$

Based on the values of the above analytical expressions and following the J&C method, the following five rules apply:

- the direction of flow is given by D (8 wind directions are used, accounting for the signs of W and S)
- if  $|Z| < F$ , there is a purely advective or directional type, defined according to Rule 1 (N, NE, E, SE, S, SW, W and NW)
- if  $|Z| > 2F$ , there is a cyclonic type (C) if  $Z > 0$ , or anti-cyclonic (A) if  $Z < 0$
- if  $F < |Z| < 2F$ , there is a hybrid type, depending on the sign of Z (Rule 3) and the direction of the flow obtained from Rule 1 (CN, CNE, CE, CSE, CS, CSW, CW, CNW, AN, ANE, AE, ASE, AS, ASW, AW and ANW)
- if  $F < 4.8$  and  $|Z| < 4.2$ , there is an indeterminate type (U)

As indicated above, this methodology is used to classify synoptic situations at the sea level, but it can be adapted to obtain, not a classification of synoptic situations based on two levels (sea level and 500 hPa), but rather an idea of the behaviour of the independent variables (direction and strength of flow, and vorticity) at an above-ground elevation, in this case, 500 hPa. The methodology used consists in applying the formulas explained above for the calculation of the J&C variables, but using the geopotential elevation at 500 hPa rather than the atmospheric pressure at the surface. In this adaptation, the variables F and Z cannot be expressed in the same units or with the same ranges of magnitude as for the surface analysis, as their calculation is based on geopotential data, from geopotential elevations at 500 hPa, but they do reference the above-ground flow behaviour (negative or positive vorticities, moderate or severe intensity of flow, etc.).

For the four observatories selected, the 3 years which yielded the extreme values of both higher and lower fractal dimensions were chosen. Then, the differences (significant at 95%) between the years in terms of frequency of weather types at the surface and the behaviour of D, F and Z, both at the surface and at 500 hPa were evaluated. In this way,

a synoptic significance can be assigned to the concept of fractal dimension based on the location of the observatory.

### 3 Results

#### 3.1 Grouping based on the fractal dimension

The FD values were determined for the 48 selected observatories, corresponding to the slope of the regression line that links the logarithmic values of the extent of various periods considered ( $\ln(I)$ ) on the x-axis, with the logarithmic values of the number of those periods in which some precipitation occurred ( $\ln(N)$ ). The FD values for the 48 observatories are shown in Table 1 along with Pearson’s  $R^2$  values which, as can be seen, are very high. The FD values oscillate between a maximum of 1.6039 at Lugo Airport and a minimum of 1.4499 at Ibiza Airport, and the  $R^2$  values oscillate between 0.9998 in Cuenca and 0.9853 at the Barcelona Airport.

These FD were compared with simulated values obtained from the random generation of N values. The goodness-of-fit showed values of MAE, RMSE (Fig. 4a) and ME (Fig. 4b)

**Table 1** FD and  $R^2$  values for the 48 observatories in the study

Observatory	FD	$R^2$	Observatory	FD	$R^2$
A Coruña	1.5629	0.9994	Málaga CMT	1.5595	0.9959
Albacete	1.4941	0.997	Málaga Puerto	1.5376	0.9943
Alicante	1.4710	0.991	Menorca	1.4680	0.9945
Ávila	1.5000	0.9971	Monflorite	1.5223	0.9906
Badajoz	1.5183	0.9988	Ourense	1.5704	0.9995
Barcelona Aerop.	1.5070	0.9853	Palma	1.4988	0.994
Bárdenas	1.4933	0.9959	Pamplona	1.5487	0.9988
Bilbao	1.5827	0.9997	Porreres	1.4966	0.9952
Cáceres	1.5464	0.9983	Madrid Retiro	1.5432	0.9981
Calamocha	1.4805	0.9946	Ronda	1.5832	0.9982
Castello Empu- ries	1.5160	0.9968	Salamanca	1.5075	0.9986
Castellón	1.5075	0.9878	San Vicente	1.5839	0.9996
Córdoba	1.5605	0.9983	Segovia	1.5105	0.9976
Coria	1.5644	0.9997	Soria	1.5190	0.9991
Cuenca	1.5468	0.9998	Tárrega	1.4730	0.9895
Granada	1.5941	0.9981	Teruel	1.4856	0.9909
Ibiza	1.4499	0.9893	Toledo	1.5047	0.9963
Jaca	1.5848	0.9985	Tortosa	1.5160	0.9933
Jaén	1.5573	0.9893	Utiel	1.5058	0.9986
Jávea	1.5101	0.9938	Valencia	1.5258	0.9921
La Seu Urgell	1.5030	0.9953	Valladolid	1.5261	0.9967
León	1.5578	0.9938	Vitoria	1.5559	0.9988
Logrono	1.4961	0.9943	Zamora	1.5020	0.9967
Lugo	1.6039	0.9996	Zaragoza	1.5154	0.9914

**Fig. 4** Statistical estimates of comparison between the original and simulated FD values for the 48 stations. **a** mean absolute error (MAE), root mean squared error (RMSE) and **b** mean error (ME)

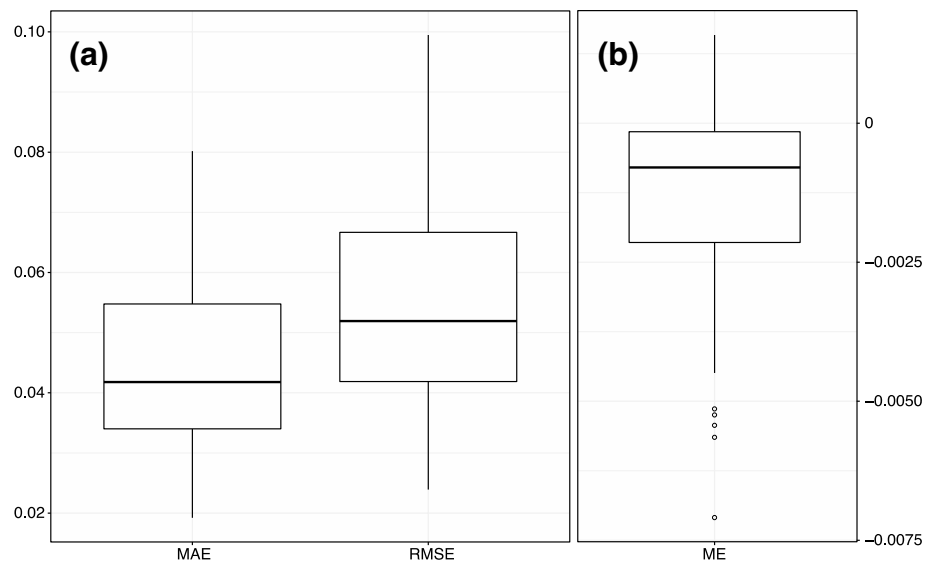


**Table 2** Central values for each cluster and significance of the differences

Variable	Cluster 1	Cluster 2	Cluster 3	Cluster 4	p value
Latitude	41.944	40.506	37.916	41.100	0.000
Longitude	-5.936	1.994	-4.855	-1.533	0.000
FD	1.545	1.494	1.551	1.521	0.001

near to zero, which means that there were not meaningful differences between observed and simulated. The mean MAE of 0.045, the mean RMSE of 0.056 and the mean ME of  $-0.0017$  between simulated and observed were much lower than the mean difference of  $\pm 0.1$  between the observed FD values (mean value of 1.5264). Although this difference between FD values could seem negligible, it is significant in comparison with simulations.

A cluster analysis that accounts for the latitude and longitude of the observatories was performed based on these values, and the FD values obtained are presented in the above table. This procedure uses a multivariate analysis, such as the cluster analysis, with the aim of differentiating the various observatories into groups with a high degree of external heterogeneity and internal homogeneity. The final centres of the three variables considered for each cluster are listed in Table 2. As can be seen, the differences between the factors considered in each cluster are significant ( $> 99\%$ ), which demonstrates external heterogeneity and internal homogeneity. The groupings are as shown in Table 3 and Fig. 5.

After the 1000 iterations to compute simulated clusters with randomly rearranged FD values, the comparison with the original groups showed that the clusters are not the same

**Table 3** Groupings of the observatories according to the various clusters

Cluster 1	Cluster 2	Cluster 3	Cluster 4
A Coruña	Albacete	Barcelona Aeropuerto	Córdoba
Ávila	Alicante	Castello Empuries	Granada
Badajoz	Bárdenas	La Seu Urgell	Jaén
Cáceres	Bilbao	Menorca	Málaga CMT
Coria	Calamocha	Palma	Málaga Puerto
León	Castellón	Porreres	Ronda
Lugo	Cuenca	Tàrrega	
Ourense	Ibiza	Tortosa	
Madrid Retiro	Jaca		
Salamanca	Jávea		
San Vicente	Logroño		
Segovia	Monflorit		
Toledo	Pamplona		
Valladolid	Soria		
Zamora	Teruel		
	Utiel		
	Valencia		
	Vitoria		
	Zaragoza		

in any simulation. The mean coincidence of each cluster group between the original and the iterated cluster analysis by stations (Fig. 6a) was lower than the 25%. When we consider the percentage of stations that coincides with the original clusters (Fig. 6b), the average of all of them is near to zero, and especially in clusters 3 and 4 with isolated cases with complete coincidence (the number of stations in these

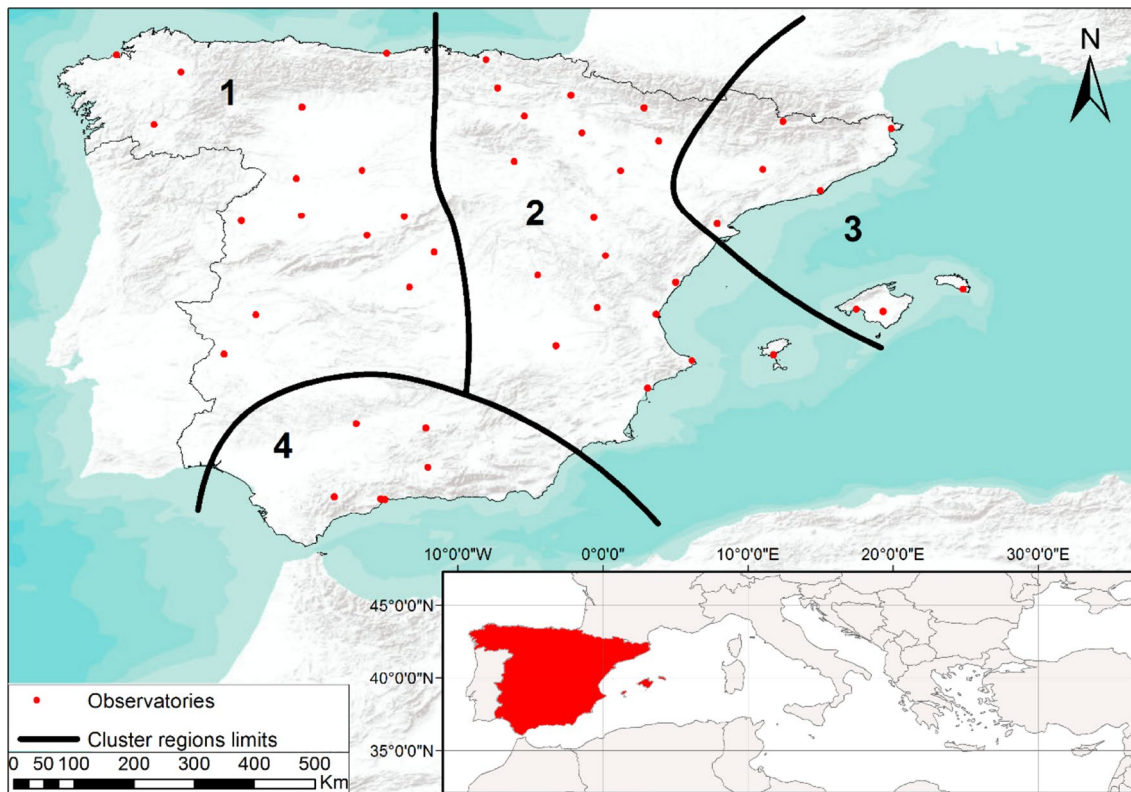


**Fig. 5** Stations grouping together after the cluster analysis

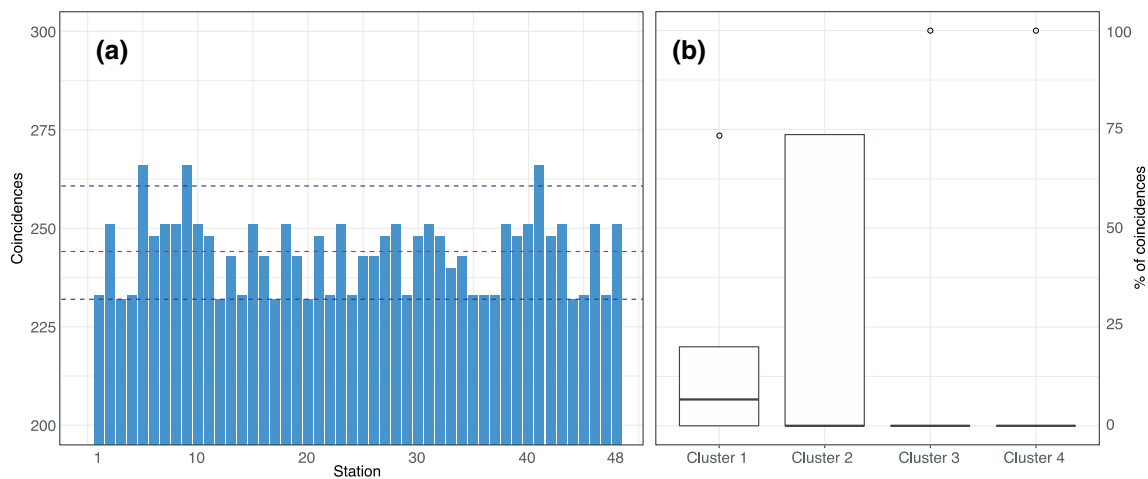


**Fig. 6 a** Number of cluster coincidences by stations between observed and simulated in the cluster analysis (blue bars) after 1000 iterations. Red dashed line shows the mean number of coincidences

and upper and lower dashed blue lines show the 95th and 5th percentile, respectively. **b** Boxplot of the percentage of coincident stations by clusters in the same analysis

original clusters are very much lower than 1 and 2). The iterated cluster analysis showed that the grouping is not only geographic. Longitude and latitude could have more

influence in cluster 1 but not exclusively. The clustering mainly depends on the FD values.

The observatories at A Coruña, Castellón, Palma and Jaen were selected as being representative of clusters 1, 2, 3 and 4,



**Table 4** Years and extreme FD values for the four observatories selected

	A Coruña		Castellón		Palma		Jaén	
	Year	FD	Year	FD	Year	FD	Year	FD
Maximum FD values	2000	1.6160	2002	1.5321	2002	1.5344	1996	1.6065
	2001	1.5957	2004	1.5626	2006	1.5368	2009	1.5987
	2006	1.5968	2006	1.5346	2010	1.5385	2010	1.6385
Minimum FD values	1998	1.5359	1995	1.4190	1995	1.3979	1995	1.4917
	2004	1.5370	1999	1.4649	1999	1.4380	1998	1.4718
	2007	1.4930	2009	1.4380	2005	1.4105	2007	1.5054

**Table 5** Frequency (%) of the weather types for the reference period 1995–2010

J&C type	%	J&C type	%
A	19.23	CS	0.53
AE	2.17	CSE	1.10
AN	1.48	CSW	1.01
ANE	1.54	CW	1.75
ANW	1.45	E	9.62
AS	0.79	N	4.63
ASE	1.24	NE	5.57
ASW	0.99	NW	4.83
AW	1.57	S	1.60
C	11.27	SE	3.88
CE	2.30	SW	3.24
CN	2.09	W	4.83
CNE	2.04	U	7.16
CNW	2.09		

respectively, as they are the observatories with the most complete and homogeneous precipitation series in each group. The years and extreme values of FD are shown in Table 4.

Based on these years, an evaluation was made of the significant synoptic differences appearing both in the types of weather at the surface and in the values of strength, direction and flow vorticity both at the surface and at 500 hPa.

### 3.2 Types of weather at the surface

As shown in Table 5, Type A is the most common in the study period (19.23%), followed by Type C (11.27%) and Type E (9.62%). The indeterminate Type U also accounts for a considerable number with 7.16% of the days, as does the purely advective types of the first and fourth quadrants (W, NW, N and NE), with a total of 29.47%.

**Table 6** Cases and percentage of each J&C weather type in years with extreme FD values at the A Coruña observatory

J&C types	Number of cases with highest FD values	%	Number of cases with lowest FD values	%
<b>A</b>	<b>827</b>	<b>18.86</b>	<b>920</b>	<b>20.99</b>
AE	88	2.01	90	2.05
AN	69	1.57	68	1.55
ANE	53	1.21	75	1.71
ANW	44	1.00	68	1.55
AS	28	0.64	31	0.71
ASE	68	1.55	56	1.28
<b>ASW</b>	<b>60</b>	<b>1.37</b>	<b>25</b>	<b>0.57</b>
<b>AW</b>	<b>90</b>	<b>2.05</b>	<b>60</b>	<b>1.37</b>
C	462	10.54	502	11.45
<b>CE</b>	<b>83</b>	<b>1.89</b>	<b>137</b>	<b>3.13</b>
CN	81	1.85	86	1.96
<b>CNE</b>	<b>74</b>	<b>1.69</b>	<b>113</b>	<b>2.58</b>
CNW	95	2.17	80	1.82
CS	23	0.52	18	0.41
CSE	58	1.32	42	0.96
CSW	47	1.07	23	0.52
CW	84	1.92	68	1.55
E	430	9.81	482	10.99
<b>N</b>	<b>167</b>	<b>3.81</b>	<b>220</b>	<b>5.02</b>
<b>NE</b>	<b>216</b>	<b>4.93</b>	<b>300</b>	<b>6.84</b>
NW	205	4.68	190	4.33
S	60	1.37	44	1.00
<b>SE</b>	<b>196</b>	<b>4.47</b>	<b>139</b>	<b>3.17</b>
<b>SW</b>	<b>182</b>	<b>4.15</b>	<b>79</b>	<b>1.80</b>
<b>W</b>	<b>267</b>	<b>6.09</b>	<b>159</b>	<b>3.63</b>
U	327	7.46	309	7.05

The bold font indicates statistically significant differences (p < 0.05)

### 3.3 Synoptic differences at the surface between extreme years for each observatory

#### 3.3.1 A Coruña

At the surface, based on the proportions comparison test, significant differences (> 95%) appear in ten synoptic types

at the A Coruña observatory (Table 6). The highest FD values are associated with years in which anticyclonic situations are less frequent (18.86%) than in years with minimal FD values (20.99%). The hybrid cyclonic types are more frequent from the east (from 1.89 to 3.13%) and from the northeast (1.69–2.58%) for years with lower FD. The purely advective types with a SE component (4.47–3.17%), SW component (4.15–1.80%) and W component (6.09–3.63%) are significantly more frequent in the years with maximum FD values, which is the opposite of what occurs with a N component (3.81–5.02%) or a NE component (4.93 and 6.84%). Therefore, higher FD values are linked to a higher proportion of SW and W advective situations, while lower FD values are associated with years in which there is a greater proportion of anticyclonic situations.

For the F variable at the surface, it can be seen from the proportion comparison test that, in years with minimal FD, a significant (> 95%) increase in the frequency of situations between 5 and 7.4 m/s appears; the other categories do not exhibit significant changes. However, at 500 hPa, the changes are significant in more categories; situations with a low flow intensity are more frequent during the years

with minimal FD, while in years with maximum FD, situations with average and strong flows appear more frequently (Fig. 7).

The direction of flow at the surface exhibits significantly greater prevalence of the first quadrant (NE) in years with minimal FD values, and a higher frequency of flows in the third in years with maximum FD values. The most notable phenomenon above ground is the higher frequency of situations with a SW component in years with maximum FD.

Changes in the vorticity are not very noticeable at the surface; significant differences only appear in the intensities of negative vorticities. However, variations do exist above ground. Slightly negative vorticities are more frequent during years with maximum FD values, and slightly positive vorticities are more frequent during years with minimal FD values.

### 3.3.2 Castellón

At the surface, the significant differences in the frequency of the synoptic weather types (Table 7) occur with the purely anticyclonic types, which are more recurrent in

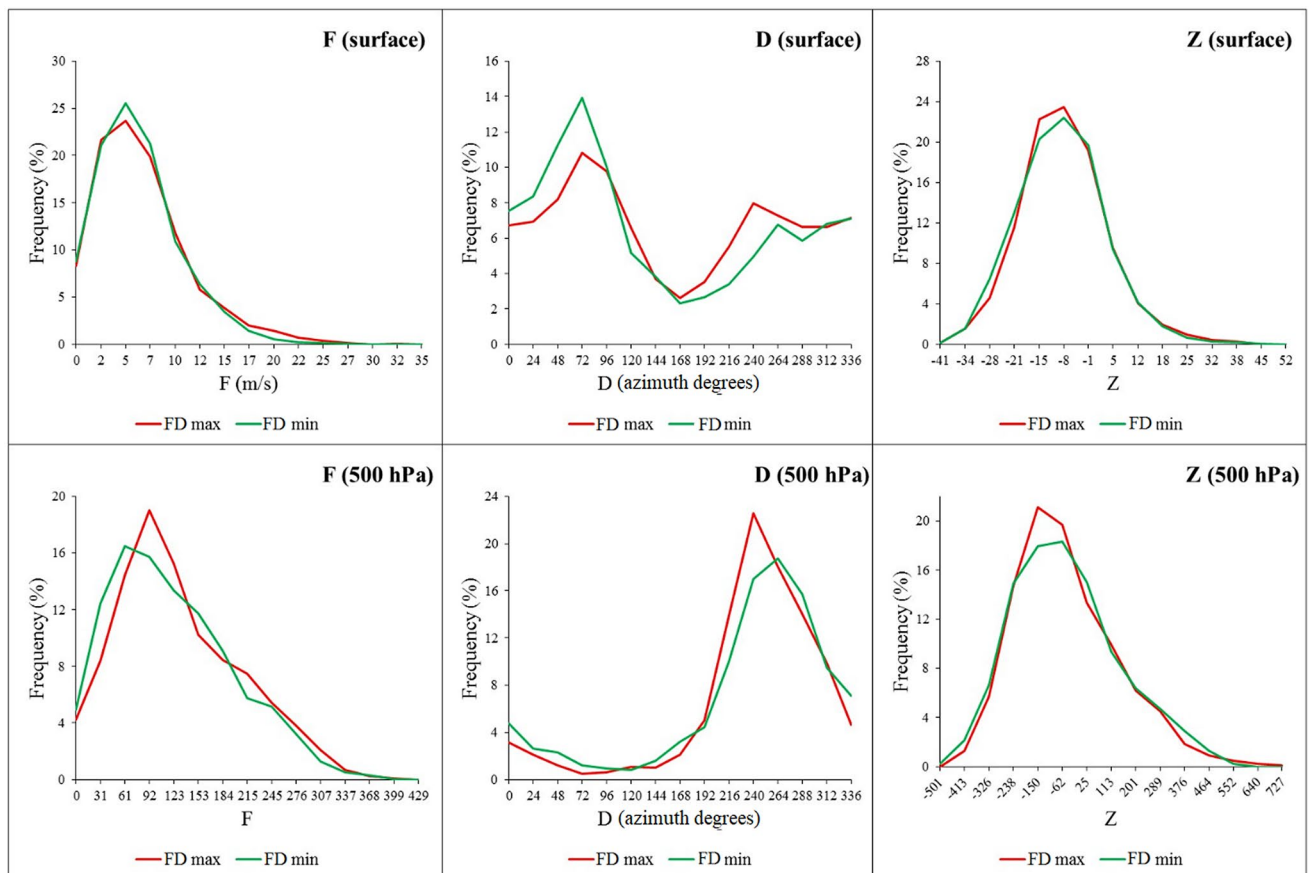


**Fig. 7** Variation of F, D and Z at the surface and at a geopotential height of 500 hPa during years with maximum (red) and minimum (green) values of FD at the A Coruña observatory

**Table 7** Cases and percentage of each J&C weather type in years with extreme FD values at the Castellón observatory

J&C types	Number of cases with highest FD values	%	Number of cases with lowest FD values	%
<b>A</b>	<b>932</b>	<b>21.26</b>	<b>793</b>	<b>18.11</b>
<b>AE</b>	<b>74</b>	<b>1.69</b>	<b>115</b>	<b>2.63</b>
AN	69	1.57	91	2.08
ANE	63	1.44	78	1.78
ANW	64	1.46	82	1.87
<b>AS</b>	<b>43</b>	<b>0.98</b>	<b>25</b>	<b>0.57</b>
<b>ASE</b>	<b>69</b>	<b>1.57</b>	<b>38</b>	<b>0.87</b>
ASW	46	1.05	57	1.30
<b>AW</b>	<b>56</b>	<b>1.28</b>	<b>86</b>	<b>1.96</b>
C	527	12.02	479	10.94
CE	127	2.90	109	2.49
CN	76	1.73	104	2.37
CNE	107	2.44	87	1.99
CNW	79	1.80	90	2.05
CS	17	0.39	18	0.41
CSE	57	1.30	40	0.91
CSW	36	0.82	47	1.07
CW	64	1.46	83	1.89
<b>E</b>	<b>380</b>	<b>8.67</b>	<b>491</b>	<b>11.21</b>
N	176	4.01	210	4.79
NE	243	5.54	205	4.68
<b>NW</b>	<b>183</b>	<b>4.17</b>	<b>227</b>	<b>5.18</b>
S	63	1.44	47	1.07
SE	146	3.33	156	3.56
SW	148	3.38	142	3.24
W	219	5.00	232	5.30
<b>U</b>	<b>320</b>	<b>7.30</b>	<b>248</b>	<b>5.66</b>

The bold font indicates statistically significant differences ( $p < 0.05$ )

years with maximum FD values (21.26 vs. 18.11%), and the purely advective types from the east (E) and from the northwest (NW), which are more frequent during years with lower FD values (8.67 vs. 11.21% and 4.17 vs. 5.18%, respectively). Significant occurrences of indeterminate Type U are also observed more frequently during years with higher FD values (7.30%) than in years with lower FD values (5.66%).

The strength of the flow, represented by the F variable, exhibits significant differences at the surface between the years with maximum FD values during which lower intensities of less than 5 m/s are more frequent, and years with minimal FD values in which moderate F intensities of up to 7.5 m/s are significantly more common. Above ground, in years with higher fractal dimensions, situations with moderate or light winds are most common, while moderately intense wind situations are more normal during years with minimal FD (Fig. 8).

There are few significant differences in the direction of flow at the surface between the two groupings of years, with situations having north-westerly flow during years with minimal FD values being the only scenario that is more common. Notably, it has been observed that, at 500 hPa, during years with maximum FD values, the flow situation from the south-west is more common than during years with minimal FD.

For its part, the vorticity at the surface exhibits few significant changes. Only situations with markedly negative vorticities occur more frequently during years with maximum FD values. Above ground, however, the situations with more marked negative vorticity are more common during years with minimal FD, whereas neutral vorticities occur more commonly during years with maximum FD.

### 3.3.3 Palma

The Palma observatory has a higher proportion of anti-cyclonic days during years with maximum FD values (19.86%) than in years with minimal FD (17.74%). Advective types from the east (E) also experience a substantial significant change, as in the first group of years, these types account for 7.99% of the years, while in the second group, and they account for 11.71%. Advective situations from the south-west also experience significant differences of 4.52–3.26% between years with maximum and minimal FD, respectively. Finally, anticyclonic hybrid types with an eastern component (AE, ANE, ASE) also experience significant differences, but these do not exceed 0.76% (Table 8).

The F variable at the surface exhibits significant differences only for moderately strong intensities of above 12.35 m/s, and is more common during years with minimal FD values. Above ground, these differences are most noticeable in light-intensity flows which are most common during years with minimal FD, and with flows of medium intensity, while flows with strong intensity occur more frequently in the years with maximum FD values (Fig. 9).

As for direction, significant changes occur at the surface primarily in the west-south-west component and are more common in years with higher FD values. At 500 hPa, however, greater differences occur. The first-quadrant directions are more common in years with lower FD values, while in the other group of years, situations from the south-west to the north-west are more common.

At the surface, negative vorticities are more common during years with minimal FD values, while markedly positive vorticities are more common in years with maximum FD values. Above ground, the most significant changes occur with markedly positive vorticities, which are more common during years with maximum FD values.

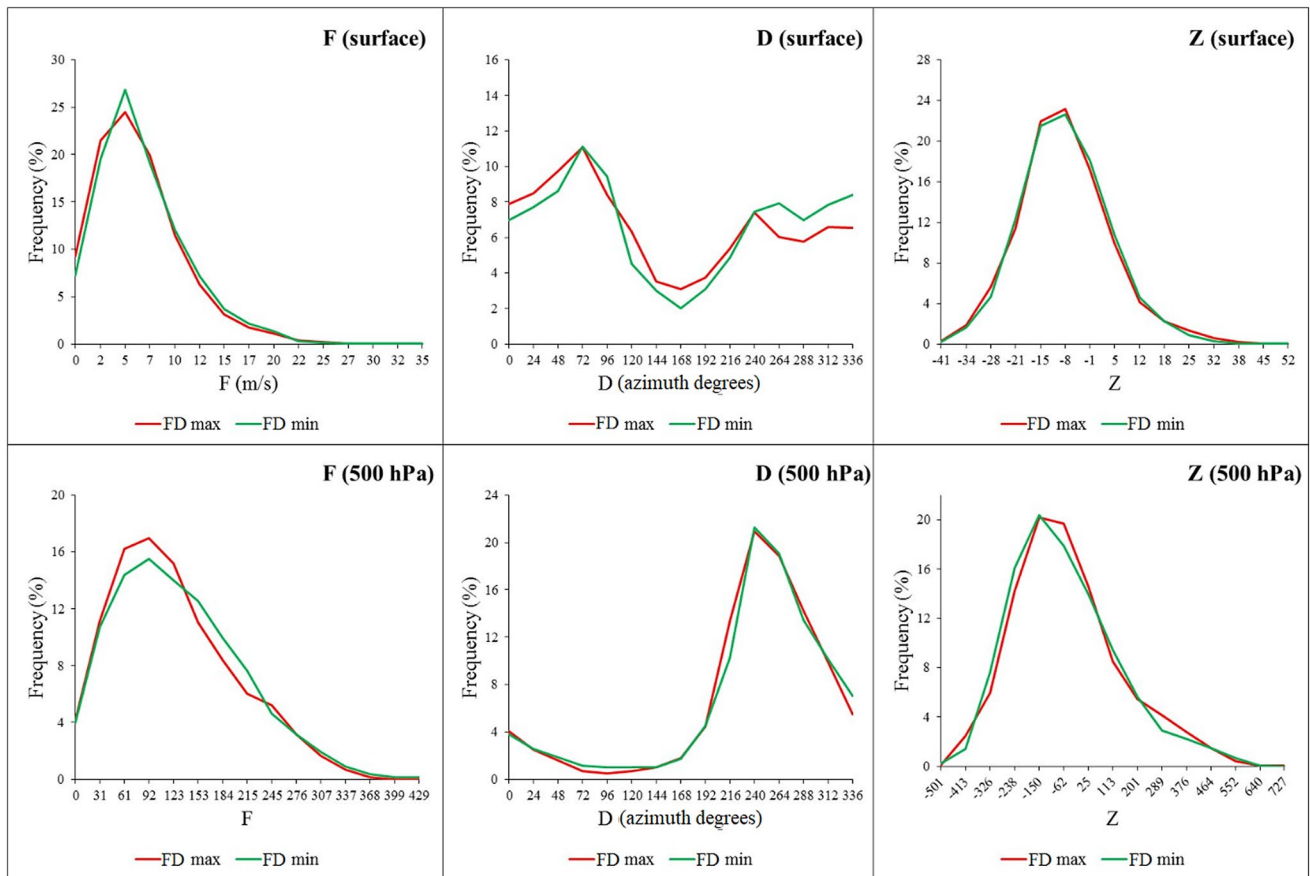


**Fig. 8** Variation of F, D and Z at the surface and at a geopotential height of 500 hPa during years with maximum (red) and minimum (green) values of FD at the Castellón observatory

### 3.3.4 Jaén

At Jaén, the anticyclonic and cyclonic types are the only ones which undergo significant changes. During years with maximum FD values, Type A is less frequent (16.95%), and Type C is more frequent (11.79%) compared with years with lower FD values, in which Type A has increased (19.84%) and C has decreased (9.57%). The N and E purely advective types also increase in the second group (from 9.72 to 11.16%, and 4.49–5.71% respectively), while the SW and indeterminate (U) types are less frequent (4.11–2.69% and 7.25–6.19%) (Table 9).

The F variable at the surface exhibits moderate intensities significantly more frequently during years with higher FD values, but the more moderate and average flows appear more frequently during years with lower FD values. The higher flow intensities, however, occur in years with maximum FD values. Above ground, mild intensities appear more commonly in the second group of years, while, similar to observations at the surface, strong intensities are more common in the first group.

At the surface, the most significant variations occur in situations with an eastern component, which are more common in years with minimal FD, in those with a south-south-western component, which exhibit more frequent significant variations during years with maximum FD values, and those with a westerly component, which again exhibit more common significant variation during years of minimal FD. At 500 hPa, flows with a westerly component are significantly more common during years with maximum FD values, with the exception of flows coming purely from the west which are significantly more common during years with minimal FD values (Fig. 10).

As for the vorticity at the surface, it is significant that during years with higher FD values, positive vorticities are more frequent, while negative vorticities are more common during years with minimal FD values. The same pattern is repeated at 500 hPa with the exception of positive vorticities which are more frequent in the second group of years.



**Table 8** Cases and percentage of each J&C weather type in years with extreme FD values at the Palma observatory

J&C types	Number of cases with highest FD values	%	Number of cases with lowest FD values	%
<b>A</b>	<b>870</b>	<b>19.86</b>	<b>777</b>	<b>17.74</b>
<b>AE</b>	<b>91</b>	<b>2.08</b>	<b>123</b>	<b>2.81</b>
AN	55	1.26	69	1.58
<b>ANE</b>	<b>47</b>	<b>1.07</b>	<b>80</b>	<b>1.83</b>
ANW	61	1.39	72	1.64
AS	51	1.16	45	1.03
<b>ASE</b>	<b>77</b>	<b>1.76</b>	<b>51</b>	<b>1.16</b>
ASW	52	1.19	46	1.05
AW	55	1.26	71	1.62
<b>C</b>	<b>487</b>	<b>11.12</b>	<b>464</b>	<b>10.59</b>
CE	98	2.24	92	2.10
CN	84	1.92	90	2.05
CNE	100	2.28	92	2.10
CNW	83	1.89	94	2.15
CS	26	0.59	17	0.39
CSE	61	1.39	41	0.94
CSW	39	0.89	39	0.89
CW	66	1.51	63	1.44
<b>E</b>	<b>350</b>	<b>7.99</b>	<b>513</b>	<b>11.71</b>
N	193	4.41	227	5.18
NE	265	6.05	264	6.03
NW	187	4.27	203	4.63
S	92	2.10	71	1.62
SE	161	3.68	156	3.56
<b>SW</b>	<b>198</b>	<b>4.52</b>	<b>143</b>	<b>3.26</b>
W	220	5.02	211	4.82
U	311	7.10	266	6.07

The bold font indicates statistically significant differences ( $p < 0.05$ )

## 4 Discussion and conclusions

The fractal dimension values obtained for the 48 observatories in the study range between 1.4499 and 1.6039. These FD values are not comparable with those of other published studies on similar study areas (Meseguer-Ruiz and Martín-Vide 2014), as the temporal resolutions of the series used are different. The resolution in the above mentioned study was 30 min, whereas the temporal resolution for this study is 10 min. This usually results in the FD data obtained in other studies being lower, as there are no data entries for intervals of 10 and 20 min, so that upon obtaining the corresponding natural logarithms and drawing the regression line, the absolute value of its slope is lower and, therefore, so is the FD value.

Breslin and Belward (1999) propose an alternative method to box-counting and Hurst's R/S analysis for calculating the fractal dimension of a temporal precipitation series based on the variation of monthly precipitation totals. The Breslin and Belward (1999) procedure, which consists of calculating the fractal dimension based on precipitation intervals instead of boxes, enables the calculation of the fractal dimension on a monthly basis, but not at a 10-min resolution, as many of the values of the series are null and are also closely spaced; therefore, the variation in this type of series would often be null.

The FD values obtained for Tunisia in Ghanmi et al. (2013) are comparable to those of this study, as they were calculated based on precipitation series at a 5-min resolution following a box-counting method. These values cluster around 1.44, which makes them very similar to those found in areas of the Spanish mainland with less precipitation (Levante, south-eastern Iberian Peninsula and the Ebro valley) and the Balearic Islands (1.4499 in Ibiza), which are regions in which the climate is similar to that of Tunisia, with dry and warm summers and mild, moderately rainy winters. The analysis of the 4 stations tends to show that few of the hybrids have significant differences. The value obtained in the study of Oñate Rubalcaba (1997) presents high difference with those obtained in this study. This could be explained, first of all, by the different time resolutions considered, annual in the first case, 10-min in the present work. Such a difference can also be explained because of the different method used to calculate the fractal dimension, Hurst exponent vs. box counting method.

In short, it can be concluded that the fractal dimension values in temporal series in the Iberian Peninsula and the Balearic Islands depend on the location and rainfall at the observatory. The highest value was found at the Lugo Airport observatory (1.6039), and the lowest value at Ibiza Airport (1.4499). At lower FD values, the property of self-similarity was fulfilled, to a large extent, in the temporal distribution of precipitation, and conversely, at greater FD values, it was fulfilled to a lesser extent; this finding coincides with the results presented in Selvi and Selvaraj (2011). In addition, the FD values links to precipitation totals have not been studied.

The regional differentiation of the Spanish mainland, carried out as a function of FD, coincides with the results of various studies (Rodríguez-Puebla and Nieto 2010; Rodríguez-Solà et al. 2016) which delineate a northern region in which rainfall is associated with the arrival of Atlantic squalls corresponding to cyclonic types, which penetrate the mainland and see a decrease in the rainfall contribution. These situations barely bring precipitation

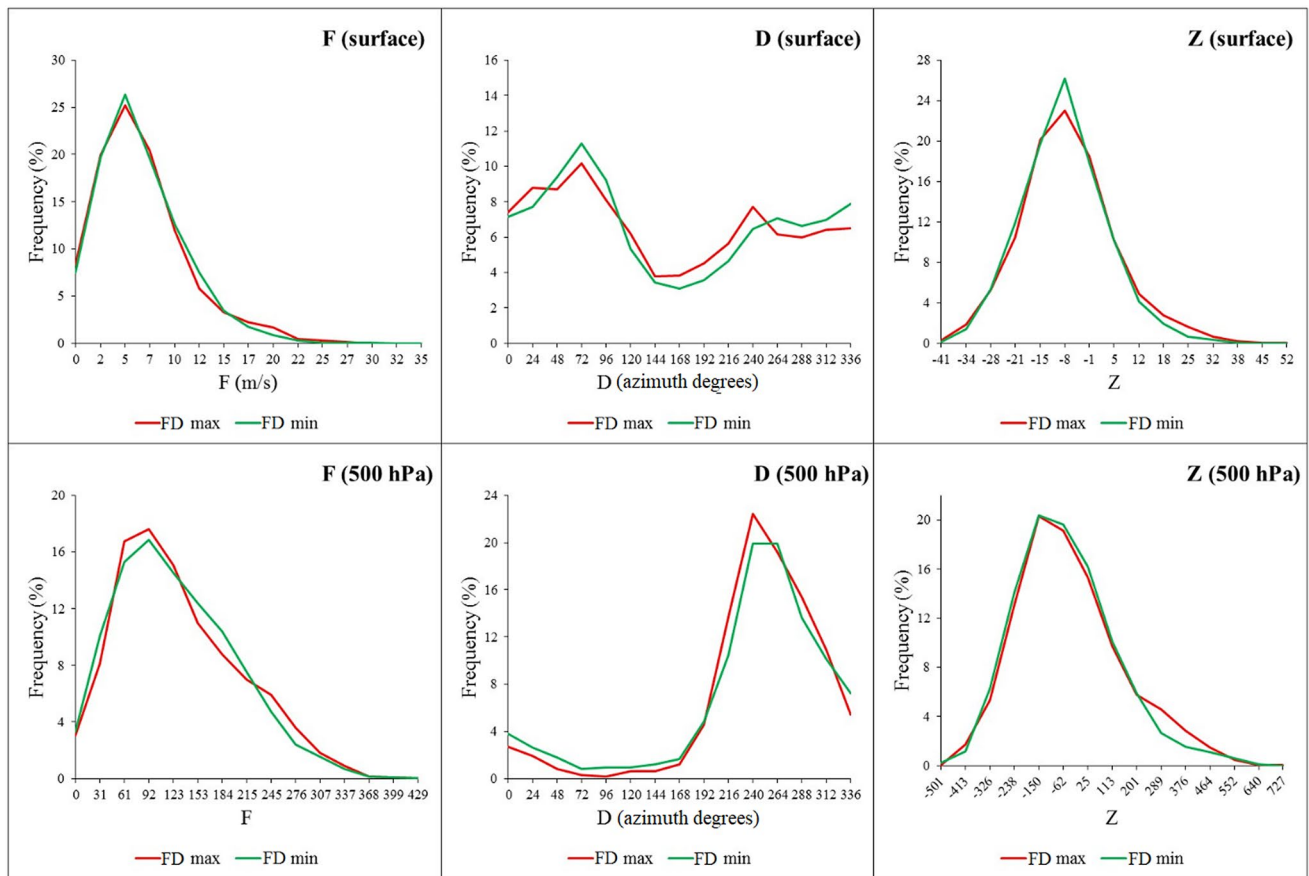


**Fig. 9** Variation of F, D and Z at the surface and at a geopotential height of 500 hPa during years with maximum (red) and minimum (green) values of FD at the Palma observatory

into Mediterranean Spain, where rain is linked to easterly storms or to the settling of squalls in the Gulf of Leon, in the western Mediterranean. In the south, rainfalls are associated with squalls settled in the Alboran Sea or off the coast of Cadiz, and circulate through the Guadalquivir valley, where episodes of rain usually wind down.

When comparing the results obtained from the list of J&C weather types with those obtained in other studies in a coincident study area (Spellman 2000; Grimalt et al. 2013), there are significant differences in the frequencies of the weather types which have a higher occurrence throughout the year (A, C, U, NE, E, W). Type A occurs at a frequency of 23.37% in the study of Spellman (2000), at 21% for Grimalt et al. (2013) and at 19.23% in the present study. The frequencies of Type C (14.58, 19 and 11.27%) are also different, as are those of Type NE (6.73, 3.1 and 5.57%), those of Type E (4.32, 2.2 and 9.62%), those of Type W (4.33, 3.4 and 4.83%), and especially those of Type U (18.14, 27 and 7.16%, respectively). The results obtained by Rasilla

Álvarez (2003) also differ slightly from those obtained in this study, and as it concerns a hybrid classification (with objective properties, Principal Component Analysis, as well as subjective properties), the results are not comparable. In other areas of the world, the proportions obtained are similar in terms of the prevalence of anticyclonic types (Pepin et al. 2011; Sarricolea et al. 2014), but have little or even no Type U. This is due to the geographical properties of the study area which has a quasi-inland sea to the east, a phenomenon which does not occur in other parts of the world with a Mediterranean climate, and frequently occurring, insignificantly contracted pressure fields during the summer.

The differences with respect to the Spellman (2000) study have two principal causes; first, the grid used in the study from 2000 had 9 points as opposed to the 16 that were used in this study, so the area covered is greater and, therefore, provides different pressure gradients. Another explanation, which particularly affects Type U, is that in the first study, a threshold of 6, below which the indeterminate type

**Table 9** Cases and percentage of each J&C weather type in years with extreme FD values at the Jaén observatory

J&C types	Number of cases with highest FD values	%	Number of cases with lowest FD values	%
<b>A</b>	<b>743</b>	<b>16.95</b>	<b>869</b>	<b>19.84</b>
AE	113	2.58	102	2.33
AN	76	1.73	61	1.39
ANE	61	1.39	72	1.64
ANW	66	1.51	72	1.64
AS	29	0.66	40	0.91
ASE	34	0.78	65	1.48
ASW	61	1.39	31	0.71
AW	56	1.28	83	1.89
<b>C</b>	<b>517</b>	<b>11.79</b>	<b>419</b>	<b>9.57</b>
CE	104	2.37	116	2.65
CN	98	2.24	93	2.12
CNE	85	1.94	97	2.21
CNW	86	1.96	84	1.92
CS	33	0.75	23	0.53
CSE	42	0.96	46	1.05
CSW	43	0.98	32	0.73
CW	82	1.87	64	1.46
<b>E</b>	<b>426</b>	<b>9.72</b>	<b>489</b>	<b>11.16</b>
<b>N</b>	<b>197</b>	<b>4.49</b>	<b>250</b>	<b>5.71</b>
NE	255	5.82	279	6.37
NW	266	6.07	195	4.45
S	67	1.53	66	1.51
SE	157	3.58	162	3.70
<b>SW</b>	<b>180</b>	<b>4.11</b>	<b>118</b>	<b>2.69</b>
W	189	4.31	181	4.13
<b>U</b>	<b>318</b>	<b>7.25</b>	<b>271</b>	<b>6.19</b>

The bold font indicates statistically significant differences ( $p < 0.05$ )

is defined, was used for the strength and vorticity of flow. Another study (Goodess and Jones 2002) states that the threshold of 6 is correct for the British Isles as proposed in the original methodology (1977), but for the Iberian Peninsula, it must be reduced to 4.8 and 4.2 for the strength and vorticity, respectively, as the circulation is less vigorous in the latter case. The same is true regarding the work of Grimalt et al. (2013). It may be interesting to choose a finer grid in the future to better cover the heavy precipitation events that are much more localized.

The grid proposed in this paper is displaced  $5^\circ$  to the east, which results in a higher probability of recording barometric

swamp situations than the grid which is presented in the Spellman (2000) study. Moreover, the smaller the space in which the J&C methodology is applied, the more difficult it will be to identify the barometric gradient; therefore, it is common for the frequency of the U type to increase. The 16-point grid also provides a more reliable reflection of the dominant flows in the study area.

In view of the results obtained in the application of J&C in the fractal dimensions, and being aware that the sample of years used is not desirable in terms of its length, we can state that the synoptic significance of higher or lower fractal dimension values depends firstly on the region in which the observatory is located and therefore, on the atmospheric mechanisms which give rise to precipitation. To summarize, it could be argued that the higher fractal dimensions in the Atlantic half of the peninsula are associated with weather types in which cyclonic and advective types have prevailed most frequently, as these are the weather types which give rise to rainfall in this part of the study area. The greatest frequency of this type of mechanism implies that precipitation is more frequent and random, and is furthest removed from the property of perfect self-similarity in the temporal distribution of precipitation. In contrast, when anticyclonic types dominate more, precipitation is scarce and, therefore, its occurrence is more sporadic and concentrated, fulfilling self-similarity to a greater extent and yielding lower FD values. However, in the Mediterranean part of the Iberian Peninsula, the high FD values high are associated with a higher frequency of Type A, because if a general anticyclonic situation occurs, the flows from the west and the Atlantic squalls will not affect the Iberian Peninsula. Nevertheless, with that situation in the Mediterranean, flows or local mechanisms that give rise to precipitation may operate in this area (Lionello 2012). The years with lower fractal dimension values are associated with flows from the first quadrant, which cause rains in the eastern mainland, but they are not very frequent or recurring throughout the year; therefore the property of self-similarity is less clear. Due to the temporal resolution available for the precipitation data, it is possible that this variable records variations based on the microclimatic properties of the site under consideration. These are processes of low spatial dimension which are not reflected in a grid of the dimensions available for this study, and for which one would have to consider applying poorly developed latitudinal and longitudinal grids.

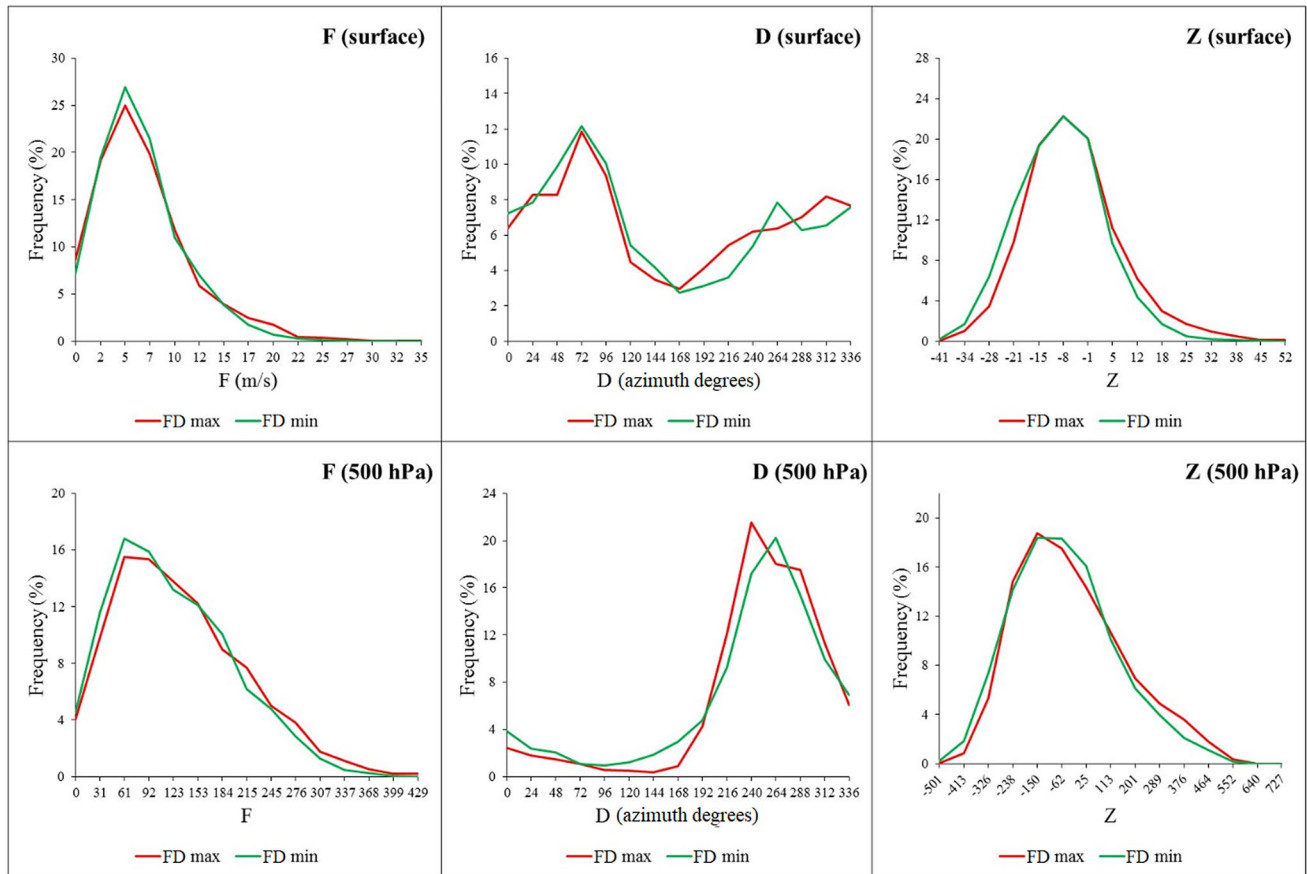


**Fig. 10** Variation of F, D and Z at the surface and at a geopotential height of 500 hPa during years with maximum (red) and minimum (green) values of FD at the Jaén observatory

**Acknowledgements** The authors want to thank the UTA-Mayor Project 5755-17 (Universidad de Tarapacá). This research is also included in the investigation program of the Climatology Group from the University of Barcelona (2014SGR300, Catalan Government). The authors would finally like to thank the ERA Interim Reanalysis Project and the Agencia Estatal de Meteorología for the data sets.

## References

- Amaro IR, Demey JR, Macchiavelli R (2004) Aplicación del Análisis R/S de Hurst para estudiar las propiedades fractales de la precipitación en Venezuela. *Interiencia* 29(011):617–620
- Breslin MC, Belward JA (1999) Fractal dimensions for rainfall time series. *Math Comput Simulat* 48:437–446. [https://doi.org/10.1016/S0378-4754\(99\)00023-3](https://doi.org/10.1016/S0378-4754(99)00023-3)
- Casanueva A, Rodríguez-Puebla C, Frías MD, González-Reviriego N (2014) Variability of extreme precipitation over Europe and its relationships with teleconnection patterns. *Hydrol Earth Syst Sc* 18:709–725. <https://doi.org/10.5194/hess-18-709-2014>
- De Luis M, Brunetti M, Gonzalez-Hidalgo JC, Longares LA, Martin-Vide J (2010) Changes in seasonal precipitation in the Iberian Peninsula during 1946–2005. *Global Planet Chang* 74:27–33. <https://doi.org/10.1016/j.gloplacha.2010.06.006>
- Dee DP, Uppala SM, Simmons AJ et al (2011) The ERA-Interim reanalysis: configuration and performance of the data assimilation system. *Q J R Meteorol Soc* 137:553–597. <https://doi.org/10.1002/qj.828>
- Del Río S, Herrero L, Fraile R, Penas A (2011) Spatial distribution of recent rainfall trends in Spain (1961–2006). *Int J Climatol* 31:656–667. <https://doi.org/10.1002/joc.2111>
- Demuzere M, Werner M (2006) Jenkinson-Collision classifications as a method for analyzing GCM-scenario pressure fields, with respect to past and future climate change and European simulated mineral dust deposition. Dissertation, Max Planck Institute for Biogeochemistry
- Dunkerley D (2008) Rain event properties in nature and in rainfall simulation experiments: a comparative review with recommendations for increasingly systematic study and reporting. *Hydrol Process* 22:4415–4435. <https://doi.org/10.1002/hyp.7045>
- Dunkerley DL (2010) How do the rain rates of sub-events intervals such as the maximum 5- and 15-min rates ( $I_5$  or  $I_{30}$ ) relate to the properties of the enclosing rainfall event? *Hydrol Process* 24:2425–2439. <https://doi.org/10.1002/hyp.7650>
- Esteban P, Martin-Vide J, Mases M (2006) Daily atmospheric circulation catalogue for Western Europe using multivariate techniques. *Int J Climatol* 26:1501–1515. <https://doi.org/10.1002/joc.1391>



- Faranda D, Messori G, Yiou P (2017) Dynamical proxies of North Atlantic predictability and extremes. *Sci Rep-UK* 7:41278. <https://doi.org/10.1038/srep41278>
- Gao M, Hou X (2012) Trends and multifractal analysis of precipitation data from Shandong peninsula, China. *Am J Environ Sci* 8(3):271–279
- García-Marín AP (2007) Análisis multifractal de series de datos pluviométricos en Andalucía. PhD Thesis, University of Córdoba, Córdoba
- García-Marín AP, Jiménez-Hornero FJ, Ayuso-Muñoz JL (2008) Universal multifractal description of an hourly rainfall time series from a location in southern Spain. *Atmosfera* 21(4):347–355
- Ghanmi H, Bargaoui Z, Mallet C (2013) Investigation of the fractal dimension of rainfall occurrence in a semi-arid Mediterranean climate. *Hydrol Sci J* 58(3):483–497. <https://doi.org/10.1080/02626667.2013.775446>
- Gonzalez-Hidalgo JC, Lopez-Bustins JA, Štěpánek P, Martín-Vide J, de Luis M (2009) Monthly precipitation trends on the Mediterranean fringe of the Iberian Peninsula during the second half of the twentieth century (1951–2000). *Int J Climatol* 29:1415–1429. <https://doi.org/10.1002/joc.1780>
- González-Hidalgo JC, De Luís M, Raventós J, Sánchez JR (2003) Daily rainfall trend in the Valencia Region of Spain. *Theor Appl Climatol* 75:117–130. <https://doi.org/10.1007/s00704-002-0718-0>
- Goodchild MF (1980) Fractals and the accuracy of geographical measures. *Math Geol* 12(2):85–98. <https://doi.org/10.1007/BF01035241>
- Goodchild MF, Mark DM (1987) The fractal nature of geographic phenomena. *Ann Assoc Am Geogr* 77(2):265–278. <https://doi.org/10.1111/j.1467-8306.1987.tb00158.x>
- Goodess CM, Jones PD (2002) Links between circulation and changes in the characteristics of Iberian rainfall. *Int J Climatol* 22:1593–1615. <https://doi.org/10.1002/joc.810>
- Grimalt M, Tomàs M, Alomar G, Martín-Vide J, Moreno-García MDC (2013) Determination of the Jenkinson and Collison's weather types for the western Mediterranean basin over 1948–2009 period. Temporal analysis. *Atmosfera* 26:75–94. [https://doi.org/10.1016/S0187-6236\(13\)71063-4](https://doi.org/10.1016/S0187-6236(13)71063-4)
- Hastings HM, Sugihara G (1994) Fractals: a user's guide for the natural sciences. Oxford University Press, Oxford
- Jenkinson AF, Collison P (1977) An initial climatology of gales over the North Sea. Synoptic Climatology Branch Memorandum no 62, Bracknell. Meteorological Office, London
- Jones PD, Hulme M, Briffa KR (1993) A comparison of Lamb circulation types with an objective classification scheme. *Int J Climatol* 13:655–663. <https://doi.org/10.1002/joc.3370130606>
- Jones PD, Harpham C, Briffa KR (2013) Lamb weather types derived from reanalysis products. *Int J Climatol* 33:1129–1139. <https://doi.org/10.1002/joc.3498>
- Kalauzi A, Cukic M, Millá H, Bonafoni S, Biondi R (2009) Comparison of fractal dimension oscillations and trends of rainfall data from Pastaza Province, Ecuador and Veneto, Italy. *Atmos Res* 93:673–679. <https://doi.org/10.1016/j.atmosres.2009.02.007>
- Khan MS, Siddiqui TA (2012) Estimation of fractal dimension of a noisy time series. *Int J Comput Appl* 45(10):1–6
- Kutiél H, Trigo RM (2014) The rainfall regime in Lisbon in the last 150 years. *Theor Appl Climatol* 118:387–403. <https://doi.org/10.1007/s00704-013-1066-y>
- Lamb HH (1972) British Isles weather types and a register of daily sequence of circulation patterns, 1861–1971. Geophysical Memoir 116. HMSO, London
- Langousis A, Veneziano D, Furcolo P, Lepore C (2009) Multifractal rainfall extremes: theoretical analysis and practical estimation. *Chaos Soliton Fract* 39:1182–1194. <https://doi.org/10.1016/j.chaos.2007.06.004>
- Liberato MLR (2014) The 19 January 2013 windstorm over the North Atlantic: large-scale dynamics and impacts on Iberia. *Weather Clim Extremes* 5–6:16–28. <https://doi.org/10.1016/j.wace.2014.06.002>
- Linderson M (2001) Objective classification of atmospheric circulation over southern Scandinavia. *Int J Climatol* 21:155–169. <https://doi.org/10.1002/joc.604>
- Lionello P (2012) The climate of the Mediterranean region. From the past to the future. Elsevier Insights, London
- López Lambrano AA (2014) Análisis multifractal y modelación de la precipitación. PhD Thesis, Universidad Autónoma de Querétaro, Querétaro
- Lovejoy S, Mandelbrot BB (1985) Fractal properties of rain, and a fractal model. *Tellus A* 37A:209–232. <https://doi.org/10.1111/j.1600-0870.1985.tb00423.x>
- Malinverno A (1990) A simple method to estimate the fractal dimension of a self-affine series. *Geophys Res Lett* 17(11):1953–1956. <https://doi.org/10.1029/GL017i011p01953>
- Mandelbrot BB (1977) The fractal geometry of nature. W H Freeman and Company, New York
- Martín-Vide J, Lopez-Bustins JA (2006) The western Mediterranean oscillation and rainfall in the Iberian Peninsula. *Int J Climatol* 26:1455–1475. <https://doi.org/10.1002/joc.1388>
- Martín-Vide J, Sanchez Lorenzo A, Lopez-Bustins JA, Cordobilla MJ, Garcia-Manuel A, Raso JM (2008) Torrential rainfall in northeast of the Iberian Peninsula: synoptic patterns and WeMO influence. *Adv Sci Res* 2:99–105. <https://doi.org/10.5194/asr-2-99-2008>
- Martín-Vide J (2002) Aplicación de la clasificación sinóptica automática de Jenkinson y Collison a días de precipitación torrencial en el este de España. In: Cuadrat JM, Vicente SM, Saz MA (eds) La información climática como herramienta de gestión ambiental. Universidad de Zaragoza, Zaragoza, pp 123–127
- Martín-Vide J (2004) Spatial distribution of a daily precipitation concentration index in Peninsular Spain. *Int J Climatol* 24:959–971. <https://doi.org/10.1002/joc.1030>
- Meseguer-Ruiz O, Martín-Vide J (2014) Análisis de la fractalidad temporal de la precipitación en Cataluña, España (2010). *Investigaciones Geográficas* 47:41–52
- Meseguer-Ruiz O, Martín-Vide J, Olcina Cantos J, Sarricolea P (2017a) Análisis y comportamiento espacial de la fractalidad temporal de la precipitación en la España peninsular y Baleares (1997–2010). *B Asoc Geogr Esp* 73:11–32. <https://doi.org/10.21138/bage.2407>
- Meseguer-Ruiz O, Olcina Cantos J, Sarricolea P, Martín-Vide J (2017b) The temporal fractality of precipitation in mainland Spain and the Balearic Islands and its relation to other precipitation variability indices. *Int J Climatol* 37(2):849–860. <https://doi.org/10.1002/joc.4744>
- Nunes SA, Romani LAS, Avila AMH, Coltri PP, Traina C, Cordeiro RLF, De Sousa EPM, Traina AJM (2013) Analysis of large scale climate data: how well climate change models and data from real sensor networks agree? In: Schwabe D, Almeida V, Glaser H, Baeza-Yates R, Moon S (ed) proceedings of the IW3C2 WWW 2013 conference, IW3C2 2013, Rio de Janeiro, pp 517–526
- Oñate Rubalcaba JJ (1997) Fractal analysis of climatic data: annual precipitation records in Spain. *Theor Appl Climatol* 56:83–87. <https://doi.org/10.1007/BF00863785>
- Osborn TJ, Jones PD (2000) Air flow influences on local climate: observed United Kingdom climate variations. *Atmos Sci Lett*. <https://doi.org/10.1006/asle.2000.0017>
- Osborn TJ, Conway D, Hulme M, Gregory J, Jones PD (1999) Air flow influences on local climate: observed and simulated mean relationships for the United Kingdom. *Clim Res* 13:173–191. <https://doi.org/10.1006/asle.2000.0013>

- Peitgen HO, Jürgens H, Saupe D (1992) *Chaos and fractals: new frontiers of science*. Springer, New York
- Pepin NC, Daly C, Lundquist J (2011) The influence of surface versus free air decoupling on temperature trend patterns in the western United States. *J Geophys Res* 116:D10109. <https://doi.org/10.1029/2010JD014769>
- Pérez SP, Sierra EM, Massobrio MJ, Momo FR (2009) Análisis fractal de la precipitación anual en el este de la Provincia de la Pampa. *Argentina Revista de Climatología* 9:25–31
- Philipp A, Beck C, Huth R, Jacobeit J (2014) Development and comparison of circulation type classifications using the COST 733 dataset and software. *Int J Climatol*. <https://doi.org/10.1002/joc.3920>
- Post P, Truija V, Tuulik J (2002) Circulation weather types and their influence on temperature and precipitation in Estonia. *Boreal Environ Res* 7:281–289
- Ramos AM, Trigo RM, Liberato MLR (2016) Ranking of multi-day extreme events over the Iberian Peninsula. *Int J Climatol*. <https://doi.org/10.1002/joc.4726>
- Rasilla Álvarez DF (2003) Aplicación de un método de clasificación sinóptica a la Península Ibérica. *Investigaciones Geográficas* 30: 27–45
- Rehman S (2009) Study of Saudi Arabian climatic conditions using Hurst exponent and climatic predictability index. *Chaos Soliton Fract* 39:499–509. <https://doi.org/10.1016/j.chaos.2007.01.079>
- Rehman S, Siddiqi AH (2009) Wavelet based Hurst exponent and fractal dimensional analysis of Saudi climatic dynamics. *Chaos Soliton Fract* 40:1081–1090. <https://doi.org/10.1016/j.chaos.2007.08.063>
- Reiser H, Kutiel H (2010) Rainfall uncertainty in the Mediterranean: intraseasonal rainfall distribution. *Theor Appl Climatol* 100:105–121. <https://doi.org/10.1007/s00704-009-0162-5>
- Rodríguez R, Casas MC, Redaño A (2013) Multifractal analysis of the rainfall time distribution on the metropolitan area of Barcelona (Spain). *Meteorol Atmos Phys* 121:181–187. <https://doi.org/10.1007/s00703-013-0256-6>
- Rodríguez-Puebla C, Nieto S (2010) Trends of precipitation over the Iberian Peninsula and the North Atlantic Oscillation under climate change conditions. *Int J Climatol* 30:1807–1815. <https://doi.org/10.1002/joc.2035>
- Rodríguez-Solà R, Casas-Castillo MC, Navarro X, Redaño Á (2016) A study of the scaling properties of rainfall in Spain and its appropriateness to generate intensity-duration-frequency curves from daily records. *Int J Climatol*. <https://doi.org/10.1002/joc.4738>
- Sáenz J, Zubillaga J, Rodríguez-Puebla C (2001) Interannual variability of winter precipitation in northern Iberian Peninsula. *Int J Climatol* 21:1503–1513. <https://doi.org/10.1002/joc.699>
- Sarricolea P, Meseguer-Ruiz O, Martín-Vide J (2014) Variabilidad y tendencias climáticas en Chile central en el período 1950–2010 mediante la determinación de los tipos sinópticos de Jenkinson y Collison. *B Asoc Geogr Esp* 64:227–247
- Sarricolea P, Meseguer-Ruiz O, Martín-Vide J, Outeiro L (2017) Trends in the frequency of synoptic types in central-southern Chile in the period 1961–2012 using the Jenkinson and Collison synoptic classification. *Theor Appl Climatol*. <https://doi.org/10.1007/s00704-017-2268-5>
- Selvi T, Selvaraj S (2011) Fractal dimension analysis of Northeast monsoon of Tamil Nadu. *Univ J Environ Res Technol* 1(2):219–221
- Soriano C, Fernández A, Martín-Vide J (2006) Objective synoptic classification combined with high resolution meteorological models for wind mesoscale studies. *Meteorol Atmos Phys* 91:165–181. <https://doi.org/10.1007/s00703-005-0133-z>
- Spellman G (2000) The use of an index-based regression model for precipitation analysis on the Iberian peninsula. *Theor Appl Climatol* 66:229–239. <https://doi.org/10.1007/s007040070027>
- Spellman G (2016) An assessment of the Jenkinson and Collison synoptic classification to a continental mid-latitude location. *Theor Appl Climatol*. <https://doi.org/10.1007/s00704-015-1711-8>
- Sprott JC (2003) *Chaos and time-series analysis*. Oxford University Press, Oxford
- Tang L, Chen D, Karlsson PE, Gu Y, Ou T (2009) Synoptic circulation and its influence on spring and summer surface ozone concentrations in southern Sweden. *Boreal Environ Res* 14:889–902
- Trigo R, Dacamara CC (2000) Circulation weather types and their influence on the precipitation regime in Portugal. *Int J Climatol* 20:1559–1581. [https://doi.org/10.1002/1097-0088\(20001115\)20:13<1559::AID-JOC555>3.0.CO;2-5](https://doi.org/10.1002/1097-0088(20001115)20:13<1559::AID-JOC555>3.0.CO;2-5)
- Trigo RM, Añel J, Barriopedro D, García-Herrera R, Gimeno L, Nieto R, Castillo R, Allen MR, Massey N (2013) The record winter drought of 2011–12 in the Iberian Peninsula, in explaining extreme events of 2012 from a climate perspective. *Bull Am Meteorol Soc* 94(9):S41–S45
- Trigo RM, Ramos C, Pereira SS, Ramos AM, Zêzere JL, Liberato MLR (2015) The deadliest storm of the 20th century striking Portugal: flood impacts and atmospheric circulation. *J Hydrol*. <https://doi.org/10.1016/j.jhydrol.2015.10.036>
- Tuček P, Marek L, Paszto V, Janoška Z, Dančák M (2011) Fractal perspectives of GIScience based on the leaf shape analysis. In: *GeoComputation conference proceedings*, pp 169–176
- Veneziano D, Langousis A, Furcolo P (2006) Multifractality and rainfall extremes: a review. *Water Resour Res*. <https://doi.org/10.1029/2005WR004716>
- Vicente-Serrano SM, Trigo RM, Lopez-Moreno JI, Liberato MLR, Lorenzo-Lacruz J, Begueria S, Moran-Tejeda E, El Kenawy A (2011) Extreme winter precipitation in the Iberian Peninsula in 2010: anomalies, driving mechanisms and future projections. *Clim Res* 46(1):51–65. <https://doi.org/10.3354/cr00977>
- Wolf M (2014) Nearest-neighbor-spacing distribution of prime numbers and quantum chaos. *Phys Rev E* 89(2):022922, 1–11. <https://doi.org/10.1103/PhysRevE.89.022922>
- Wolf A, Swift JB, Swinney HL, Vastano JA (1985) Determining Lyapunov exponents from a time series. *Phys D* 16(3):285–317. [https://doi.org/10.1016/0167-2789\(85\)90011-9](https://doi.org/10.1016/0167-2789(85)90011-9)
- Zhou X (2004) Fractal and multifractal analysis of runoff time series and stream networks in agricultural watersheds. Virginia Polytechnic Institute and State University, Virginia